Chinese Chemical Letters 34 (2023) 107573

Contents lists available at ScienceDirect

Chinese Chemical Letters

journal homepage: www.elsevier.com/locate/cclet

A three-dimensional biomimetic microfluidic chip to study the behavior of hepatic stellate cell under the tumor microenvironment

Jingjing Kuang[a,1], Wei Sun[a,1], Min Zhang[b,*], Lu Kang[a], Shenglong Yang[a], Hongyang Zhang[a], Yuerong Wang[a], Ping Hu[a,*]

[a] *Shanghai Key Laboratory of Functional Materials Chemistry, School of Chemistry and Molecular Engineering, East China University of Science and Technology, Shanghai 200237, China*

[b] *Engineering Research Centre of Pharmaceutical Process Chemistry, Ministry of Education, School of Pharmacy, East China University of Science and Technology, Shanghai 200237, China*

ARTICLE INFO

Article history:
Received 25 October 2021
Revised 17 May 2022
Accepted 28 May 2022
Available online 31 May 2022

Keywords:
Interstitial flow
Hypoxia
Microfluidic
Tumor microenvironment
Behavior

ABSTRACT

In this paper, we designed a three-dimensional cell co-cultured microfluidic chip, which generated interstitial flow and oxygen gradient to simulate the complex tumor microenvironment. It consisted of five parallel cell culture channels and one hypoxic channel. These channels were constructed for the culture of mouse liver tumor cells (Hepa1-6), mouse liver stellate cells (JS-1), the simulation of extracellular matrix, complex biochemical factors (hypoxia and interstitial flow), and the supply of cellular nutrients. The 3D-interstitial flow-hypoxia model was used to study the behavior of JS-1 cells under the effect of tumor microenvironment (TME). The results showed that by co-cultured with Hepa1-6 cells, hypoxia of Hepa1-6 cells, and adding TGF-β1 by interstitial flow, the migration of JS-1 cells could be promoted. Similarly, activated JS-1 cells could led to the epithelial-mesenchymal transformation in co-cultured Hepa1-6 cells, which secreted more TGF-β1.

Solid tumors function differently from normal cells in stromal interactions and intercellular interactions [1]. 3D culture system can make certain spatial arrangements among cells, and realize certain tissue and organ functions through mutual regulation of basic physiological activities of cells such as cell proliferation, apoptosis, migration and differentiation [2,3]. New cell culture platforms based on various 3D cell culture technologies have emerged successively, such as biological scaffolds [4], sandwich cell co-cultured method [5], bioreactor [6], microfluidic chip technology [7,8]. Microfluidic chip technology has become an important technology to simulating TME for 3D culture *in vitro* due to the micron-level fluid control. It can regulate the growth of *in vitro* cells and various cell behaviors through space-controlled co-culture, perfusion culture and controllable signal gradient [9–11].

Due to the irregular vascular network caused by the rapid growth of tumors, there are often a large number of hypoxic cells in tumors. The oxygen content of these cells decreases with the increase of the distance from blood vessels, which presents a radial oxygen gradient. Hypoxia can affect various behaviors of cells, such as accelerating cell migration [12], promoting stem cell differentiation [13], promoting angiogenesis [14], promoting tumor cell growth [15] and inducing drug resistance of tumor cells [16,17]. Therefore, simulated an accurate oxygen environment is of great significance for the study of tumor [18]. In recent years, microfluidic techniques have been used to establish a variety of hypoxia models *in vitro*. Lin *et al.* [19] designed an integrated double-layer chip for cell co-culture under different oxygen concentrations and realized on-line monitoring biomarkers modulation of cervical cancers. Shih *et al.* [20] achieved an oxygen gradient ranging from 1% to 19% in the chip with oxygen absorption reagent, and realized patterned culture of human umbilical vein endothelial cell.

Fluid flow in living organisms can be roughly divided into blood flow and interstitial flow (IF, the flow of fluid between tissues). IF as a kind of movement driven by hydrostatic pressure and osmotic pressure, IF can generate shear stress in tissues, which can induce cell differentiation [21–23]. IF can also change cell phenotype and migration behavior by forming a concentration gradient of autocrine and paracrine cytokines in the cell microenvironment [24]. It plays an important role in the spatial distribution of soluble biomolecular in tissues, angiogenesis and nutrient supply in tumor [25–27]. IF is considered to be an important catalyst in the

* Corresponding authors.
E-mail addresses: zhangm@ecust.edu.cn (M. Zhang), huping@ecust.edu.cn (P. Hu).

[1] These authors contributed equally to this work.

https://doi.org/10.1016/j.cclet.2022.05.087

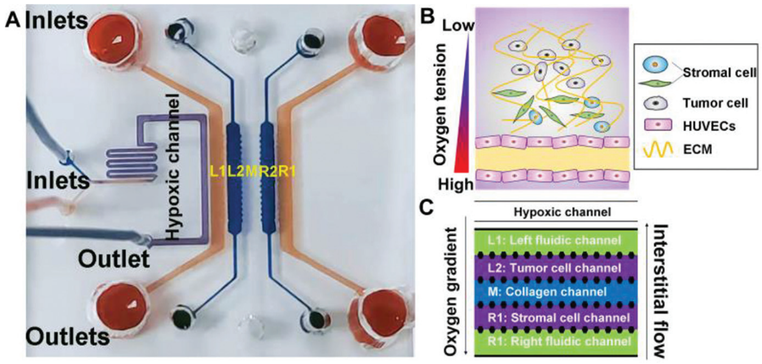

Fig. 1. The schematic diagram of the microfluidic chip for simulating simplified TME. (A) Image of the chip filled with red and blue dyes showing the mixture and flow in the chip. (B) The schematic diagram of simplified TME. (C) The 3D co-cultured module in microfluidic chip.

TME to promote cancer metastasis, which changes the adhesion of tumor cells and the property of extracellular matrix (ECM). Kalchman *et al.* [28] established a 3D hydrogel structure in the central channel of a three-channel chip, and inoculated HepG2/HLE cells to the edge of the hydrogel structure. Then forward/reverse IF was introduced into the chip. It was found that the cell migration rate was higher under reverse osmosis. Song *et al.* [29] co-cultured human lymphoma cells (U937), human umbilical vein endothelial cells (HUVECs) and human breast cancer cells (MDA-MB-231) in a chip to study the interaction between cells. The results showed that U937 cells transformed into tumor-associated macrophages under the effects of tumor cells and IF, and the transformed U937 cells and tumor cells further promoted the vascular sprouting of HUVECs.

Using microfluidic technology to create 3D-IF-hypoxic model *in vitro* is helpful to understand the TME. Hsu reported a microfluidic platform to study mass transport which was controlled by adjust different downstream positions of long microfluidic channels in 3D tissue culture, and demonstrated that vasculogenesis could be independently stimulated by interstitial flow or hypoxic conditions [30]. Galie and Stegemann studied the paracrine effects of co-cultured implanted MSC on resident myofibroblasts in a controlled biochemical and mechanical environment which included oxygen tensions under 2.5% O_2 (hypoxia) incubator and exposed to either 5% strain at a frequency of 1 Hz or 10 µL/min of interstitial fluid flow [31]. Few studies have been conducted on stromal cells which play an important role in TME. Furthermore, transforming growth factor-β1 (TGF-β1) has been found to be associated with cancer invasion, progression, and metastases [32–34] in patients with malignancies. In this paper, we established a hypoxic-IF-3D co-cultured model to study the behavior of hepatic stellate cells, which play an important role in the matrix of liver tumors. The migration behavior of hepatic stellate cells under various conditions and the effect of TGF-β1 on migration were also investigated.

TME plays a key role in tumor formation, growth and invasion. To simulate the TME in microfluidic chip, we simplified and integrated environmental factors of TME into our microfluidic chip. The microfluidic chip was consisted of a hypoxic channel and a cell culture unit of five channels (Fig. 1). The hypoxic channel was used to produce stable oxygen gradient to simulate TME. The cell culture unit was separated by a series of hexagon micropillars with a side length of 100 µm. The micropillars helped resist the leakage of media into adjacent channels. L1 and R1 channels simulated the tumor vessels and transported nutrients. Hepa1-6 tumor cell and JS-1 stromal cell were cultured in cell channels L2 and R2 and their paracrine effects were studied. M channel could be used as a 3D ECM barrier to separate the two kinds of cells. Collagen type I was used in channel L2, R2 and M to form concentration gradient of biochemical factors between tumor cell and stromal cell and reconstitute the ECM of tumor. Compared to previous studies [35,36], this chip can be used to establish a more accurate liver tumor model *in vitro* considering cell interaction, ECM, hypoxia and interstitial flow. Moreover, the co-cultured of cells in different regions is more conducive to the behavioral characterization of cells.

In order to study the diffusion trend of soluble factors under IF, 50 kDa FITC-glucan was selected as simulation molecule to obtain an approximate diffusion rate, for its molecular weight was similar to TGF-β1. The fluorescence image showed that FITC-glucan diffused from R1 channel to L1 channel (Figs. S1A–F in Supporting information), and the fluorescence intensity of each channel increased with time, resulting in a directional concentration gradient. After 6 h of diffusion, FITC-glucan diffused to L1 channel, and after 12 h the concentration of FITC-glucan in the chip tended to be consistent. In actual cell experiments, as cell metabolism continuously consumes the nutrients in chip, the concentration gradient should be maintained by replacing fresh medium every 12 h. The migration distance at different times is manually measured by comparing the actual chip length in image. The migration rates of FITC-glucan in chip are shown in Fig. S1G (Supporting information). The flow speed of IF decreased over time, which resulted from the decrease of the liquid level difference between channel R1 and L1 channel. The average flow speed decreased from 3.15 ± 0.56 µm/s at 2 min to 0.46 ± 0.06 µm/s at 120 min. The speed range matches that *in vitro* TME model [37], and our IF model is suitable for the simulation of TME.

The excessive deposition of ECM caused by the continuous activation of hepatic stellate cells could cause liver cancer [38]. First, we monitored the growth and morphology of JS-1 cells under mono-cultured and co-cultured with Hepa1-6 cells conditions. Increase of cell volume and cell process expansion are the characteristics of hepatic stellate cell activation [39]. The FITC-labeled phalloidin stained F-actin in cells showed the distribution of microfilament skeletons in cells. Under mono-cultured conditions, JS-1 cells are round (Fig. S2A in Supporting information), while under co-cultured conditions, JS-1 cells are elongated (Fig. S2B in Supporting information). The fluorescence quantification results of F-actin (Fig. S2C in Supporting information) showed that the expression of F-actin under co-cultured conditions increased significantly compared with mono-cultured conditions ($P < 0.05$), indicating that JS-1 cells were activated in co-cultured conditions. Increased expression of α-SMA is one of the marker factors in the activation of hepatic stellate cells. In Figs. S2D and E (Supporting information), the fluorescence intensity of α-SMA under co-cultured conditions is significantly higher than that under mono-cultured conditions. The fluorescence intensities of the two calculated by software (Fig. S2F in Supporting information) show

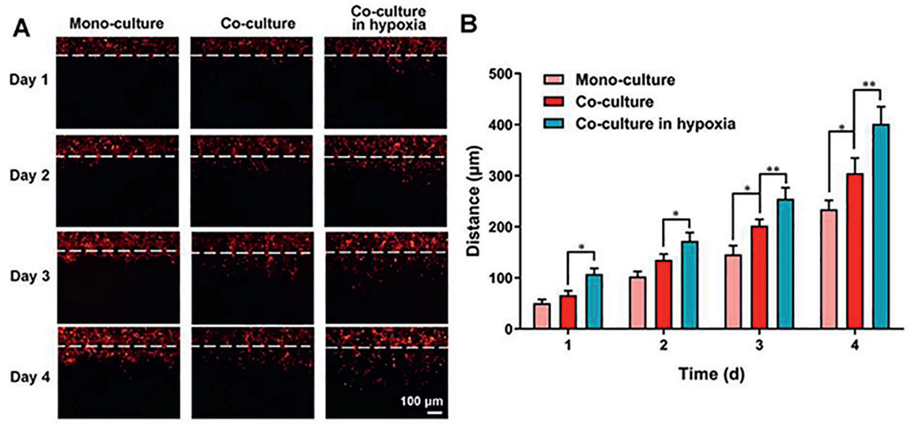

Fig. 2. Migration of JS-1 cell under the effect of hypoxic Hepa1-6 cell. (A) The fluorescent image of JS-1 cell migration under different condition. (B) Quantitative analysis of average migration distance of JS-1 cell, scale bars in (A) were all 100 μm. * $P < 0.05$, ** $P < 0.01$.

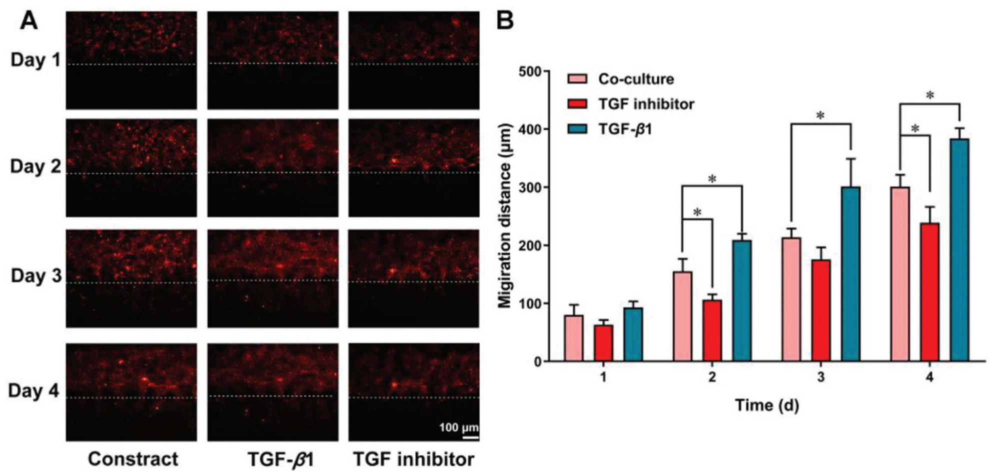

Fig. 3. The effect of TGF-β1 and TGF-β inhibitor on JS-1 cell migration. (A) The fluorescent image of JS-1 cells migration under different condition. (B) Quantitative analysis of average migration distance of JS-1 cell. Scale bars in (A) were all 100 μm. * $P < 0.05$.

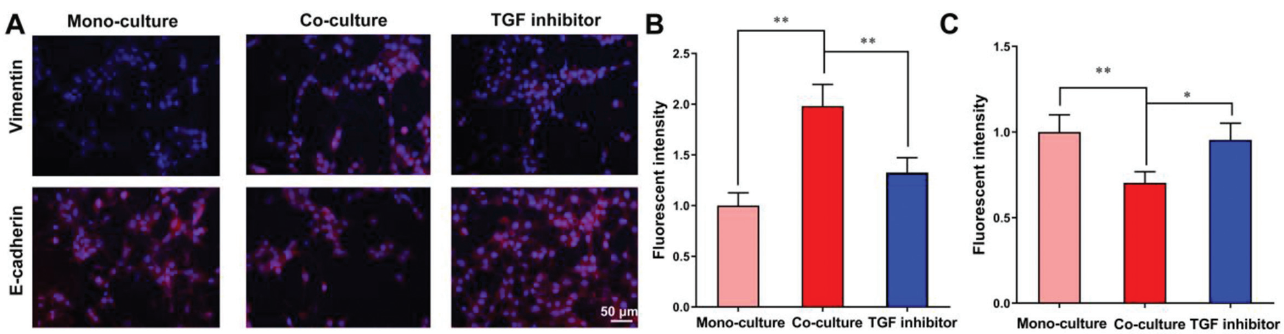

Fig. 4. Expression of EMT-related markers in Hepa1-6 cell. (A) The fluorescent images of two markers in different conditions. (B) The result of expression of Vimentin in different groups. (C) The result of expression of E-cadherin in different groups. Cells were cultured for 3 days. Data are expressed as the mean ± SE of 3 independent experiments, scale bars in (A) were all 50 μm. * $P < 0.05$, ** $P < 0.01$.

a statistical difference ($P < 0.05$), which further shows that JS-1 cells were activated under co-cultured conditions.

Cell density is also an important factor to affect tumor cell migration. After 4 days of continuous co-culture, Hepa1-6 cells and JS-1 cells both migrated to the channel M. The migration distance of JS-1 cells increased with the increase of cell density in both mono-culture group (Fig. S3A in Supporting information) and co-cultured group (Fig. S3B in Supporting information) after 4 days. There were distinct differences between low-density group, middle-density group and high-density group ($P < 0.05$), indicating that cell density can significantly affect the migration of JS-1 cells. The effect of co-culture on the migration of JS-1 cells is shown in Figs. S3C–E (Supporting information). The migration distance of mono-cultured JS-1 cells was less than that of co-cultured JS-1 cells in all cell density groups after 4 days ($P < 0.05$), indicating that co-culturing with Hepa1-6 cells could promote the migration of JS-1 cells.

Radial oxygen gradient of Hepa1-6 cells incubated in channel L2 was created by chemical oxygen absorption method to simulate the radial oxygen gradients in the organism. In order to observe JS-

1 cells directly, only the fluorescence of JS-1 cell staining is shown in Fig. 2A. It can be seen that JS-1 cells gradually migrated to the channel M in the 4-day experiment with IF condition. The data obtained by measuring the migration distance are shown in Fig. 2B. From 24 h after the experiment, the migration distance of JS-1 cells in hypoxia group was significantly higher than that in the other two groups ($P < 0.05$). All results indicated that hypoxia can further accelerate the migration of JS-1 cells in co-cultured condition.

TGF-β1 is an important molecule for regulating cell growth and differentiation. It can activate downstream signal and promote cell growth through Smad-2 and Smad-3 pathway [40]. In liver cancer tissues, TGF-β1 interacts with stromal cells and the expression of TGF-β1 increases, stimulate the activation of static hepatic stellate cells, increase the synthesis of ECM and affect proliferation, migration and differentiation.

We investigated the effect of TGF-β1 on the migration of JS-1 cells co-cultured with Hepa1-6 cell in the microfluidic chip. TGF-β1 or TGF-β1/Smad inhibitor SB431542 was added into DMEM of R1 channel, which flowed through cell culture units through IF. It can be seen in Fig. 3A that within 4 days of the experiment, JS-1 cells continuously migrated to the channel M. In the TGF-β/Smad inhibitor SB431542 group, the migration distance and migration number of JS-1 cells were smaller than those of the control group and the TGF-β1 group. In Fig. 3B, the cell migration rate of TGF-β1 group was statistically higher than those of the other groups ($P < 0.05$) after day 2, indicating that TGF-β1 can effectively promote JS-1 cell migration. In contrast, when the TGF-β/Smad inhibitor was added to the co-cultured system, the migration rate of JS-1 cells decreased significantly, and the migration distance between day 2 and day 4 was statistically different from that of the control group ($P < 0.05$), indicating that inhibition of TGF-β1 expression can reduce the rate of migration of JS-1 cells. Since the activation of JS-1 cells can promote their cell migration, the reduction of the migration rate also means that the activation of JS-1 cells is inhibited. The cytokine TGF-β1 may be the key factor leading to the acceleration and migration of JS-1 cells.

E-cadherin and Vimentin, as marker proteins of the epithelial and mesenchymal phenotypes of cells, marks the occurrence of Epithelial-mesenchymal transition (EMT) in cells [41–43]. In Fig. 4A, the red fluorescence is protein expression, and the blue fluorescence is nuclear staining. In Figs. 4B and C, it can be seen that JS-1 cell promoted the EMT of Hepa1-6 in co-cultured group. The higher fluorescence intensity of Vimentin and the lower fluorescence intensity of E-cadherin in co-cultured group indicated that the mobility of tumor cells was higher, adhesion between cells was weakened and the metastasis ability of tumor cells was enhanced. The addition of TGF-β/Smad inhibitor inhibited the expression of TGF-β1, which weakened the EMT of Hepa1-6 cells, reversing the protein expression and making it more similar to that of the mono-cultured group.

We established IF and hypoxic model on a 3D cell co-cultured microfluidic chip. The diffusion and distribution of biochemical factors across the gel channel in the chip were investigated by using 50 kDa FITC-glucan. The results showed that the glucan could reach to the co-cultured cells within 12 h under IF. In addition, we studied the behavior of JS-1 cells under IF conditions. The results showed that co-culturing with Hepa1-6 cells, hypoxia of Hepa1-6 cells and TGF-β1 all promoted the migration of JS-1 cells. The morphology of JS-1 cells in co-cultured was more elongated, the expression of F-actin and α-SMA were increased. While Hepa1-6 cells were co-cultured with JS-1 cells, the expression of EMT marker E-cadherin was decreased and the expression of Vimentin was increased. In summary, tumor cells can secrete TGF-β1 to activate the static hepatic stellate cells, then activated hepatic stellate cells promote the EMT of tumor cells to secrete more TGF-β1, thus forming a paracrine cycle. The microfluidic chip has the advantages of simple structure, convenient operation, flexible application and no need of large external equipment. By changing the cell types cultured, oxygen concentration and transported cytokines, adding cell cultured channels, the simulation of different types of TME can be adapted, providing a new strategy for tumor biology research *in vitro*. In addition, our chips have great application potential in drug discovery, drug screening, personalized medicine, and molecular mechanism research.

Declaration of competing interest

The authors declare that they have no known competing financial interests or personal relationships that could have appeared to influence the work reported in this paper.

Acknowledgment

This work was supported by the National Natural Science Foundation of China (No. 81973285).

Supplementary materials

Supplementary material associated with this article can be found, in the online version, at doi:10.1016/j.cclet.2022.05.087.

References

[1] R. Portillo-Lara, N. Annabi, Lab Chip 16 (2016) 4063–4081.
[2] K.M. Yamada, E. Cukierman, Cell 130 (2007) 601–610.
[3] F. Pampaloni, E.G. Reynaud, E.H.K. Stelzer, Nat. Rev. Mol. Cell Biol. 8 (2007) 839–845.
[4] J.L. Drury, D.J. Mooney, Biomaterials 24 (2003) 4337–4351.
[5] L. Richert, D. Binda, G. Hamilton, et al., Toxicol. Vitro 16 (2002) 89–99.
[6] M.J. Powers, K. Domansky, M.R. Kaazempur-Mofrad, et al., Biotechnol. Bioeng. 78 (2002) 257–269.
[7] I. Maschmeyer, A.K. Lorenz, K. Schimek, et al., Lab Chip 15 (2015) 2688–2699.
[8] H.C. Chang, C.H. Lin, D.E. Juang, et al., Biofabrication 11 (2019) 035024.
[9] R. Li, J.D. Hebert, T.A. Lee, et al., Cancer Res. 77 (2017) 279–290.
[10] P.J. Lee, P.J. Hung, L.P. Lee, Biotechnol. Bioeng. 97 (2007) 1340–1346.
[11] C.P. Huang, J. Lu, H. Seon, et al., Lab Chip 9 (2009) 1740–1748.
[12] J.V. Joseph, S. Conroy, K. Pavlov, et al., Cancer Lett. 359 (2015) 107–116.
[13] Q. Lin, Y.J. Lee, Z. Yun, J. Biol. Chem. 281 (2006) 30678–30683.
[14] D. Liao, R.S. Johnson, Cancer Metastasis Rev. 26 (2007) 281–290.
[15] P. Vaupel, Oncologist 9 (2004) 10–17.
[16] W.R. Wilson, M.P. Hay, Nat. Rev. Cancer 11 (2011) 393–410.
[17] P. Vaupel, A. Mayer, Cancer Metastasis Rev. 26 (2007) 225–239.
[18] B. Muz, P. de la Puente, F. Azab, A.K. Azab, Hypoxia 3 (2015) 83–92.
[19] X. Lin, Q. Chen, W. Liu, et al., Sci. Rep. 5 (2015) 1–7.
[20] H.C. Shih, T.A. Lee, H.M. Wu, et al., Sci. Rep. 9 (2019) 1–10.
[21] M.A. Swartz, M.E. Fleury, Annu. Rev. Biomed. Eng. 9 (2007) 229–256.
[22] K. Yamamoto, T. Sokabe, T. Watabe, et al., Am. J. Physiol. Heart Circ. Physiol. 288 (2005) H1915–H1924.
[23] D. Li, T. Tang, J. Lu, K. Dai, Tissue Eng. Part A 15 (2009) 2773–2783.
[24] J.K.G. Dhont, W.J. Briels, Rheol. Acta 47 (2008) 257–281.
[25] V. Vickerman, J. Blundo, S. Chung, R. Kamm, Lab Chip 8 (2008) 1468–1477.
[26] J.Y. Park, S.J. Yoo, C.M. Hwang, S.H. Lee, Lab Chip 9 (2009) 2194–2202.
[27] Q.D. Tran, D. Marcos, G. Rodriguez, Soft Matter 14 (2018) 6386–6392.
[28] J. Kalchman, S. Fujioka, S. Chung, et al., Microfluid Nanofluid 14 (2013) 969–981.
[29] C. Song, D. Gao, T.Y. Yuan, et al., Chin. Chem. Lett. 30 (2019) 1038–1042.
[30] Y.H. Hsu, M.L. Moya, P. Abiri, et al., Lab Chip 13 (2013) 81–89.
[31] P.A. Galie, J.P. Stegemann, Cytotherapy 16 (2014) 906–914.
[32] S.F. Shariat, M. Shalev, A. Menesses-Diaz, et al., J. Clin. Oncol. 19 (2001) 2856–2864.
[33] B. Jung, J.J. Staudacher, D. Beauchamp, Gastroenterology 152 (2017) 36–52.
[34] M.F. Pang, A.M. Georgoudaki, L. Lambut, et al., Oncogene 35 (2016) 748–760.
[35] Y.Q. Chen, W. Sun, L. Kang, et al., Analyst 144 (2019) 4233–4240.
[36] W. Sun, Y.Q. Chen, M.F. Wang, et al., Chin. J. Anal. Chem. 48 (2020) 180–186.
[37] B. Kramer, L. de Haan, M. Vermeer, et al., Int. J. Mol. Sci. 20 (2019) 4647.
[38] S.L. Friedman, Gastroenterology 134 (2008) 1655–1669.
[39] M.C. Nollevaux, Y. Guiot, Y. Horsmans, et al., Liver Int. 26 (2006) 182–186.
[40] S.J. Chen, W. Yuan, Y. Mori, et al., J. Invest. Dermatol. 112 (1999) 49–57.
[41] A. Smith, T.N. Teknos, Q.T. Pan, Oral Oncol. 49 (2013) 287–292.
[42] S.J. Serrano-Gomez, M. Maziveyi, S.K. Alahari , Mol. Cancer 15 (2016) 1–14.
[43] A.M. Richardson, L.S. Havel, A.E. Koyen, et al. , Clin. Cancer Res. 24 (2018) 420–432.